CFD-CAA simulations of the human phonation

Martin Lasota[1]; Petr Šidlof[1,2]
[1]Technical University of Liberec, NTI FM, Liberec, Czechia
[2]Institute of Thermomechanics, Czech Academy of Sciences, Prague, Czechia

Objectives

- This contribution deals with large-eddy simulations (LES) of 3D incompressible laryngeal flow through vocal folds followed by aeroacoustic simulations of wave propagation (human phonation) of five cardinal vowels /u, i, ɑ, o, æ/.
- Several conventional and relatively new subgrid-scale turbulence models are emloyed and their relatively sensitive impact on the flow field and aeroacoustics is described.

Introduction

Numerical simulations of phonation undoubtedly have strong potential to be applied in clinical diagnostics, treatment control, and supporting medical education.

Computer analysis can
- provide highly resolved 3D data of the flow and acoustic field for further studies, such highly resolved 3D data are infeasible by in-vivo, excised larynx, or synthetic vocal fold measurements
- improve the voice quality by tissue removal (change the geometry) for subjects suffering from various vocal fold dysfunctions,
- evaluate potential effects on voice production affected by a hypothetical implant insertion.

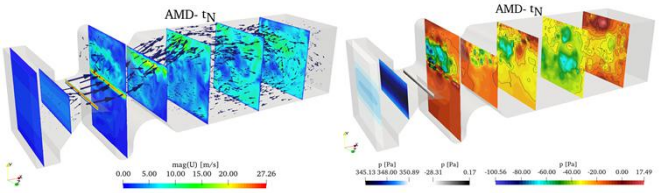

Fig. 1: 3D visualization of the **velocity** and **pressure distribution** in the human larynx during phonation.

Methods

Given the large variety of scales in the flow and acoustics, the simulation is separated into two steps:
1. CFD: computing the flow in the larynx using the finite volume method on a fine grid followed by
2. CAA: computing the sound sources and wave propagation from the larynx to the radiation space around the mouth using the finite element method on a coarse acoustic grid.

1. CFD

The continuity and momentum equations for the incompressible fluid flow, with LES filtering applied, can be written as

$$\partial_i \bar{u}_i = 0, \partial_t \bar{u}_i + \partial_j(\bar{u}_i \bar{u}_j) - \partial_j\left(\nu \partial_j \bar{u}_i\right) = -\frac{1}{\rho}\partial_i \bar{p} - \partial_j \tau_{ij},$$

where
$\bar{u}, \bar{p}$ ... filtered (large-scale) velocity and pressure,
ν, ρ ... molecular viscosity and density of air,
τ_{ij} ... subgrid-scale stress tensor.

To ensure local increasing of turbulent viscosity ν_t from small vortices into molecular viscosity ν is used the eddy-viscosity equation

$$\tau_{ij} - 0.33\,\tau_{kk} I_{ij} = -2\nu_t \bar{S}_{ij} = \nu_t\left(\partial_j \bar{u}_i + \partial_i \bar{u}_j\right),$$

where
I_{ij} ... identity matrix,
$\bar{S}_{ij}$ ... strain rate tensor,
ν_t ... turbulent (subgrid-scale) viscosity.

Here, the turbulent viscosity v_t is employed as a proportionality constant, which can be approximated in different ways, depending on the subgrid scale model.

Subgrid-scale models

- One-Equation (OE) [2]: $\nu_t = C_\nu \Delta \sqrt{k_{SGS}},$
- Wall-Adaptive Local-Eddy Viscosity (WALE) [3]: $\nu_t = (C_w \Delta)^2 \nu_t = \frac{\left(s_{ij}^d s_{ij}^d\right)^{3/2}}{\left(\bar{S}_{ij}\bar{S}_{ij}\right)^{5/2} + \left(s_{ij}^d s_{ij}^d\right)^{5/4}},$
- Anisotropic minimum dissipation (AMD) [4]: $\nu_t = C_A \frac{\max\{-(\Delta x_k \partial_k \bar{u}_i)(\Delta x_k \partial_k \bar{u}_j)\bar{S}_{ij}, 0\}}{(\partial_i \bar{u}_m)(\partial_i \bar{u}_m)},$

where
$\Delta, \Delta x_k$ ... LES filter width,
C_v, C_w, C_A ... model constants: $C_v = 0.094, C_w = 0.325, C_A = 0.3.$

2. CAA

The filtered flow quantities obtained in the first step are used in the equation for computing sound sources using PCWE [1], which has the following form

$$\frac{1}{c_0^2}\frac{\mathrm{D}^2\psi^a}{\mathrm{D}t^2} - \nabla\cdot\nabla(\psi^a) = -\frac{1}{\rho_0 c_0^2}\frac{\mathrm{D}p^{ic}}{\mathrm{D}t},$$

where
ψ^a acoustic potential
p^{ic} strain rate tensor
$1/\rho_0 c_0^2$ constant corresponds to physiological respiration at 34°C

Acoustic pressure p^a is computed from the acoustic scalar potential ψ^a

$$p^a = \rho_0 \frac{\mathrm{D}\psi^a}{\mathrm{D}t} = \rho_0 \frac{\partial \psi^a}{\partial t} + \overbrace{\rho_0 \boldsymbol{u}_0 \cdot \nabla\psi^a}^{\approx 0}.$$

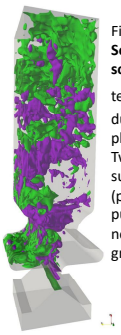

Fig. 2: **Sound source** term $\frac{\mathrm{D}p^{ic}}{\mathrm{D}t}$ during phonation. Twenty iso-surfaces (positive-purple, negative-green).

Results

Fig. 3 shows the state of the **oscillation cycle** of vocal folds glottal opening and minimum-maximum **flow rates** $(0.122 - 0.434\ \mathrm{l/s})$ during the last four simulated cycles of vocal fold oscillation. Times:
- t_N corresponds to the instant where the inferior margins of the vocal folds approach most and reduce the glottal opening to $5.58\ \mathrm{mm}^2$ $(g = 0.465\ \mathrm{mm})$.
- t_C is the maximum approach of the superior vocal fold margins, where the glottal opening drops to $4.98\ \mathrm{mm}^2$ $(g = 0.415\ \mathrm{mm})$
- t_O corresponds to the maximum glottal opening of $17.51\ \mathrm{mm}^2$ $(g = 1.459\ \mathrm{mm})$

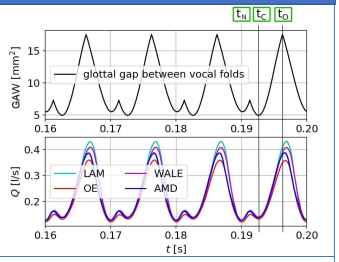

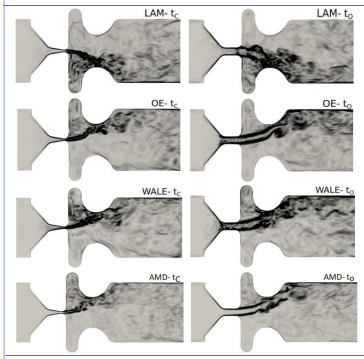

Fig. 4 represents **vorticity** fields in mid-coronal plane in range $(0{,}30000)\ \mathrm{s}^{-1}$. The supraglottal jet deflects stochastically towards either of the ventricular folds. This behavior is not a consequence of the SGS model, it is caused by the bistability of the flow in this symmetric geometry.

The simulation with the AMD model predicts low vorticity in the vicinity of the glottis. The absence of vorticity may imitate the situation in the realistic larynx where the jet is frequently stopped and renewed, and thus the turbulent eddies are forced to be dissipated.

Detailed analysis of the vorticity within the glottal region shows that the average value of vorticity in glottal region is similar for all SGS models.

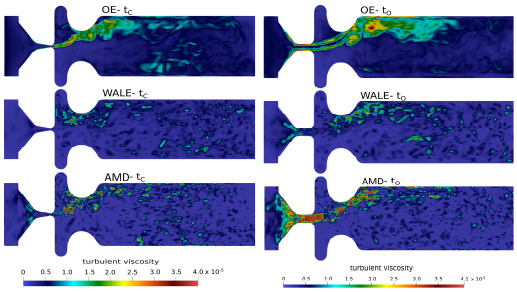

Fig. 5 shows that the **turbulent viscosity** predicted by the simulation with the OE model is high in regions of pure shear, especially within glottis. This may be the reason why the simulation with the OE model predicted most of the time the lowest intraglottal velocity. In contrast to this, WALE and AMD subgrid-scale models predicted at t_C considerably lower turbulent viscosity in the shear layers.

The fields computed by the AMD model seem to be similar to fields computed by WALE with spots of gently higher subgrid-scale viscosity. The other situation occurs at t_O when the turbulent viscosity predicted by the AMD model is around two times higher than by OE and five times higher than by WALE (only for a short time).

Fig. 6 illustrates the geometry used for aeroacoustic simulations, where from the left side are: the **PML** (perfectly matched layer) layer at inlet to guarantee that no wave reflections occur at boundaries, **VF** (vocal folds in the larynx, our CFD results), **VT** (vocal tract) and the **RZ** (radiation zone) protected by PML. MIC1 is placed 1 cm from the mouth (end of the vocal tract).

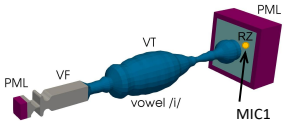

Fig. 7 shows **aeroacoustic spectrum** at MIC1 for the phonation of vowel /æ/. Total sound pressure levels (SPL) in dB are: AMD 70, LAM 67, WALE 66 and OE 61. The first formant F_1 predicted by AMD is by 13 dB higher than the formant predicted by the WALE model.
- Simulations of phonation including vowels /ɑ, æ/ computed higher $SPL(f)$ compared to vowels /u, i, o/. This can be explained by greater vocal tract passage before lips.
- For all vowels, the usage of the AMD model leads to the stronger second formant F_2, whereas the WALE model results in the stronger third formant F_3 (which is not that important to phoniatrists).

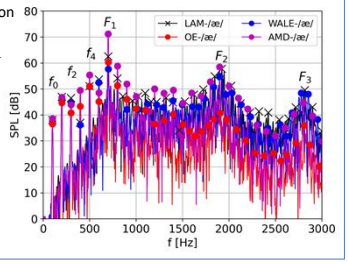

Conclusions

- This work represents the first application of the AMD model in the field of human phonation, since the AMD model had not been a part of the standard OpenFOAM package and therefore it had to be implemented by the author [5].
- The AMD model resulted in significantly higher harmonic frequencies f_N up to the 2 kHz compared to conventional subgrid-scale models. This finding could be related to known features of the AMD model: consistency with the exact subgrid-scale stress tensor τ_{ij}, no requirements on the approximation of the LES filter width Δx_k and usability on anisotropic computational meshes.
- The AMD model seems to be a very promising successor to the commonly used WALE model, although the WALE model contributes better to highlight formants F_3 and higher.

Acknowledgements

The research was supported by the Student Grant Scheme at the Technical University of Liberec through project no. SGS-2022-3016.

Contact

Martin Lasota, Ph.D.
Assistant professor, Technical University of Liberec
Studentská 2, 460 01 Liberec, Czechia
E: Martin.Lasota@TUL.cz

References

[1] Hüppe, A., and Kaltenbacher, M., Investigation of Interpolation Strategies for Hybrid Schemes in Computational Aeroacoustics, *Proc DAGA*, pp. 16–19, 2015.
[2] Davidson, L., Hybrid LES–RANS: Back Scatter from a Scale-Similarity Model Used as Forcing, *Philosophical Transactions of the Royal Society A: Mathematical, Physical and Engineering Sciences*, vol. **367**, pp. 2905–2915, 2009. DOI: 10.1098/rsta.2008.0299
[3] Nicoud, F. and Ducros, F., Subgrid-Scale Stress Modelling Based on the Square of the Velocity Gradient Tensor, *Flow, Turbulence and Combustion*, vol. **62**, pp. 183–200, 1999. DOI: 10.1023/A:1009995426001
[4] Rozema, W., Bae, H. J., Moin, P. and Verstappen, R., Minimum-Dissipation Models for Large-Eddy Simulation, *Physics of Fluids*, vol. **27**, p. 85107, 2015. DOI: 10.1063/1.4928700
[5] Lasota, M. *Large-Eddy Simulation for Aeroacoustics of Human Phonation*. PhD thesis, 2022. DOI: 10.13140/RG.2.2.26740.01925